

## Kinematic properties of the jellyfish *Aurelia* sp.

Tom Bajcar · Vlado Malačič · Alenka Malej ·  
Brane Širok

Published online: 22 September 2008  
© Springer Science+Business Media B.V. 2008

**Abstract** A new, relatively simple method for determining the kinematic properties of jellyfish is presented. The bell movement of the scyphomedusa (*Aurelia* sp.) during its pulsation cycle was analysed using computer-aided visualization. Sequences of video images of individual *Aurelia* in a large aquarium were taken using a standard video camera. The images were then processed to obtain time series of the relative positions of selected points on the surface of the medusa's bell. The duration of the bell relaxation was longer than that of the bell contraction, thereby confirming published results. In addition, the area of the exumbrellar surface of *Aurelia* increased during bell relaxation by more than 1.3-times that of the

exumbrellar surface area during the maximum contraction of the bell. The volume change during the bell pulsation cycle was also measured using the same visualization method. Significant changes, of up to 50%, in the subumbrellar cavity volume were revealed while, in contrast, the volume between the exumbrellar and subumbrellar surfaces generally remained unchanged during the entire pulsation cycle of the bell. Comparison of the time series of the exumbrellar surface area and of the subumbrellar cavity volume indicated that the change of volume takes place before the change of the surface area of the bell.

**Keywords** Scyphozoa · Computer-aided visualization · Bell pulsation

Guest editors: K. A. Pitt & J. E. Purcell  
Jellyfish Blooms: Causes, Consequences, and Recent Advances

T. Bajcar (✉) · B. Širok  
Faculty of Mechanical Engineering, University  
of Ljubljana, Aškerčeva 6, 1000 Ljubljana, Slovenia  
e-mail: tom.bajcar@fs.uni-lj.si

B. Širok  
e-mail: brane.sirok@fs.uni-lj.si

V. Malačič · A. Malej  
National Institute of Biology, Marine Biology Station  
Piran, Fornace 41, 6330 Piran, Slovenia

V. Malačič  
e-mail: malacic@mbss.org

A. Malej  
e-mail: malej@mbss.org

### Introduction

Jellyfish is a key predator in many pelagic environments worldwide. Accumulating evidence indicates an increase in the frequency and intensity of gelatinous plankton outbreaks (Brodeur et al., 1999; Hays et al., 2005; Attrill et al., 2007) as well as expansion of the range of their distribution (Graham, 2001; Graham et al., 2003; Malej & Malej, 2004). When very abundant, medusae play an important trophic role and seriously affect zooplankton populations such as ichthyoplankton and, consequently, fisheries (Purcell & Arai, 2001). The mechanics of prey capture vary between medusae, which influences prey selection

(Costello & Colin, 1995) and, consequently, impacts on the ecosystem (Malej et al., 2007). The importance of medusae jet propulsion for their displacement (swimming) and predation has been recognized since the early 1970s (Gladfelter, 1972, 1973), and our understanding of the swimming and feeding of medusae has increased substantially in last few decades (Mills, 1981; Costello & Colin, 1994; Ford et al., 1997; D'Ambra et al., 2001; Colin et al., 2006; Malej et al., 2007). Models have been developed to describe medusae jet propulsion (Daniel, 1983), swimming (Matanoski & Hood, 2006) and flow patterns generated by medusae (Dabiri et al., 2005, 2006). Costello et al. (2008) suggested two distinctive propulsion modes used by medusae: jet propulsion characteristic for small-sized organisms and rowing propulsive mode generally used by larger Scyphozoa. The differences in propulsion modes have important ecological consequences most notably on prey selection.

Among the Scyphomedusae, that recurrently appear in great densities, *Aurelia* is the most widespread and it swarms in both cold and temperate regions. Morphological characteristics affect swimming and foraging behaviour, and *Aurelia* has been classified as an oblate medusa having a rowing mode of propulsion and lower swimming performance, which create high fluid disturbance (Dabiri et al., 2005; Colin et al., 2006). The resulting fluid entrainment enhances prey encounter and affects the selection of prey organisms. Understanding the motion of *Aurelia* and the dynamics of a vortex ring (Dabiri et al., 2005) is thus very important for the species' ecology. The locomotive force depends very much on the shape and volume of the bell, the added-mass of the wake vortex tensor and the velocity of the wake.

While the Reynolds number is a parameter that relates only to the steady motion of fish, the Strouhal number relates the tail-flapping frequency to the forward speed, normalized by the amplitude of lateral motion of the tail (Lauder & Tytell, 2006). However, a similar 'generic' Strouhal number of a wake vortex was introduced for jellyfish, which is proportional to the wake vortex ratio (Dabiri et al., 2005). This is defined as the ratio of the wake vortex added-mass term to the vortex circulation term and shows whether the added-mass of wake vortices is to be considered in the swimming dynamics (the reaction or locomotive force experienced by the organism).

For a wide range of sizes of oblate medusae, the shape profile of the bell at its full contraction and relaxation is independent of size (Dabiri et al., 2005). This was demonstrated with plots of the bell profile in which dimensions were normalized by the cube root of the ejected bell fluid volume. Obviously, the geometry of the jellyfish bell plays a fundamental role. The sensitivity study of locomotion of medusae (Dabiri & Gharib, 2003) showed that, although the bell volume of medusae could be estimated from the bell profile with much greater precision than the bell aperture area, the errors of the former play a much greater role in the error of the dynamics, manifested in errors of acceleration, swimming velocity and position of medusae. A second geometric uncertainty, which was discussed in the same work, is related to the bell aperture radius. On contraction, this could be lower than the maximum radius of the bell, which is located somewhere between the bell margin and apex. This is related to the fact that the shape of the bell approaches a hemi-ellipsoid only when the medusa is in its relaxed state. Dabiri & Gharib (2003) also concluded that a single parameter was not sufficient to provide an accurate description of the animal's kinematics.

Kinematic analysis of swimming of two Cubomedusae species was done by Shorten et al. (2005) using laboratory-based digital video records. A computer analysis of the reference points identified on bell parts (nodes) enabled description of the swimming gaits used by two jellyfish species. However, the method allowed only a few nodes on the surface of the jellyfish to be identified, which were extracted manually from the image sequences.

The aim of our study was, therefore, to develop a new methodology for the research of kinematic properties of jellyfish based on computer-aided visualization. We have focussed on the velocities of the parts of the jellyfish bell that have not been addressed in previous research, and *Aurelia* was used as a model oblate medusa. The volume and surface area of the bell were also examined with this method.

## Methodology

Methodology of determining bell contour from images

Computer-aided visualization was used to determine the bell contour from images of medusae swimming.

Standard video recordings of *Aurelia* individuals were made while they were swimming in a large aquarium (Cretaquarium, Thalassocosmos, Greece). Image acquisition frequency was 25 Hz, i.e. a time difference between two successive images of 0.04 s. The methodology used to determine cyclic alteration of the medusa bell shape was as follows: *transformation* of each video image in the sequence into a binary image, with the outer contour of the *Aurelia* sp. bell clearly visible; *selection* of points along the contour of the medusa bell, where the movement is to be observed; *tracking* the time series of the spatial position of each selected point on the outer contour of the bell.

The uncertainty of the method arises mainly from the position of the medusa on the images – the medusa can approach or move away from the camera or can turn around its lateral axis (parallel to the bell aperture) during the sequence, giving an isometric view of the bell instead of its profile. Therefore, selection of the appropriate sequence of images was essential. We selected sequences other than those in which visual inspection revealed that the medusa was swimming in a plane that is obviously tilted with respect to the vertical one. The latter was deduced by observing the contour of the apex (which should on average be close to a single line) and the presence of the top of the bell (if the top was not visible, the medusa was tilted). The number of images in the sequence was selected so that the entire cycle of the periodic bell cycle of the selected medusa was included. The duration of the cycles differed and varied from about 3.5 to 5.5 s. About 130 images covered one cycle of 5.2 s (see sample images in Fig. 1).

The changes in the bell shape can be observed in the  $x$ – $y$  plane (Fig. 1). Transformation of video images into binary ones was done using the Matlab program package. The Sobel method (Sobel, 1978) for edge detection was used to determine the outer

contour of the medusa's bell. It performs a 2D spatial gradient measurement on an image. Typically, it is used to find the approximate absolute gradient magnitude at each point in an input greyscale image. The Sobel edge detector uses a pair of  $3 \times 3$  convolution masks (much smaller than an actual image), one estimating the gradient in the  $x$ -direction (columns, Fig. 1) and the other in the  $y$ -direction (rows, Fig. 1). The mask is slid over the image, manipulating one square of pixels at a time. At each point in the image, the resulting approximated gradients ( $G$ ) can be combined to give the gradient magnitude, using the Širok et al. (2002) expression:

$$G = \sqrt{G_x^2 + G_y^2}, \quad (1)$$

where  $G_x$  and  $G_y$  are gradients along the  $x$ - and  $y$ -directions. By adjusting the threshold value of the gradient  $G$ , it is possible to use this method to search for the edges between dark and bright regions (Fig. 2).

The gradient approach (Eq. 1) was applied to determine both the exumbrellar (outer) and subumbrellar (inner) contours of the medusa's bell (Fig. 3). The results were a little more uncertain in the case of the subumbrellar contour, since the grey level gradients between the subumbrellar contour and the subumbrellar cavity were smaller than those between the exumbrellar contour and the surrounding water.

#### Methodology for quantifying bell contour movement

The outer contour was next divided into an appropriate number of points, whose movements were observed. The bell was assumed to be continuously axisymmetric around its central axis, since the medusa in the selected sequences of images generally did not move in ways other than straightforward.

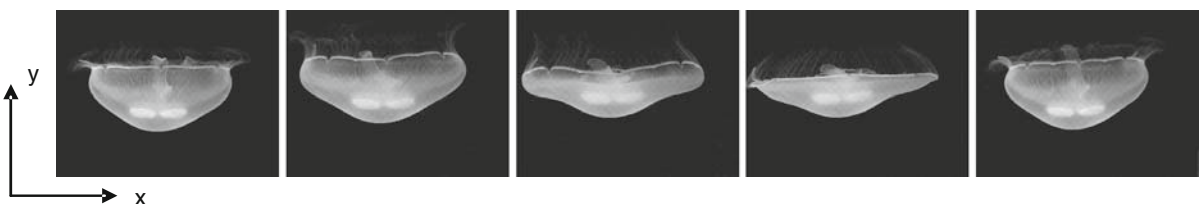


**Fig. 1** *Aurelia* sp. sample images of the sequence of changes in the form of the medusa's bell (time between two neighbouring sample images is 1.2 s)

**Fig. 2** Transformation of a video image (a) into a binary image (b) defining the outer contour of the medusa's bell

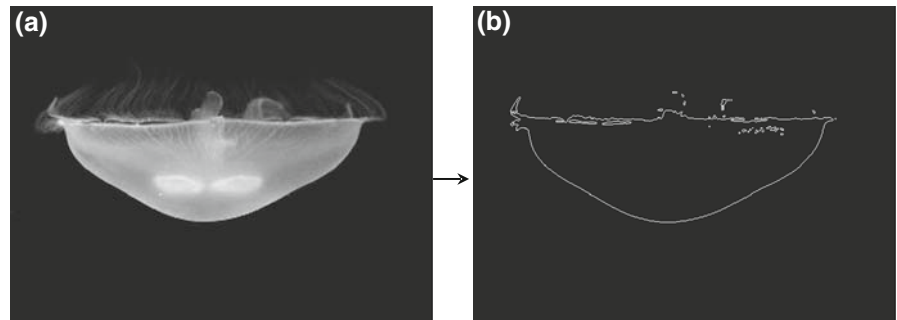


**Fig. 3** Processing of the medusa image (a) to determine the exumbrellar (outer) contour (b) and the subumbrellar (inner) contour (c)

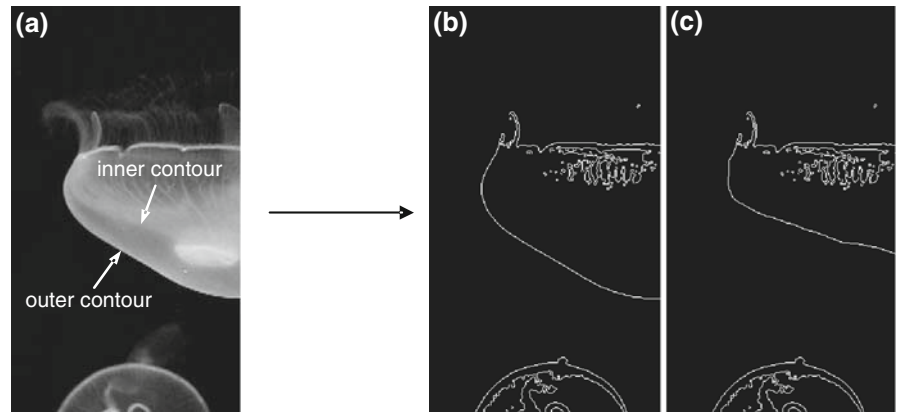
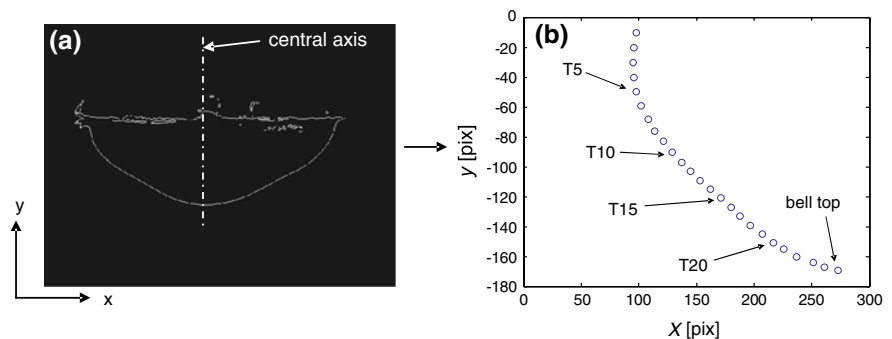


**Fig. 4** Transformation of the outer contour of the bell shape (a) into several points in the  $x$ - $y$  plane (b)



Thus, only half the bell contour (Fig. 4a) can be observed and transformed into points. The part of the outer contour that lies on the left of the central axis was chosen, since this part was not affected by the presence of other medusae behind the one observed on the binary images (Figs. 2b and 4a).

The contour on the left side of the central axis (Fig. 4a) was transformed into several points, again by using the Matlab software (Fig. 4b). Velocities of every fifth point along the contour were studied, denoted as T5, T10, T15, T20 and as the 'bell top' (Fig. 4b) for the sake of easier orientation. Our analysis focussed on the bell contour; so the points

along the tentacles at the bell margin were removed, since they were not present on all images of the sequence due to poor lighting. This procedure resulted in 25 points along the outer contour of the bell on the left side of the central axis (Fig. 4a). An effort was made to keep the points along the outer contour of the bell equidistant. However, due to the limited resolution of the images, this was not completely possible; therefore the average distance ( $l_n$ ) between two neighbouring points on the whole image sequence was  $11.4 \pm 2.2$  pixels. Pixel units, in which images are recorded, are appropriate for the measure of distances in this study, since many

important kinematic properties are extracted with non-dimensional quantities, in which space dimensions cancel out. Moreover, as was pointed out in the Introduction, the shape profile of the bell at its full contraction and relaxation is size independent (Dabiri et al., 2005).

#### Methodology for quantifying bell surface area

The intention of this study was to verify the stretching and contraction of the medusa's bell during the whole bell pulsation cycle. For this purpose, a computer-aided visualization method, similar to the one described above, was applied to determine the length of the outer bell contour, as depicted in Figs. 2b and 4a. Axisymmetry of the medusa's bell was again assumed, so only the left half of the bell was processed on each image (Fig. 4a). However, the contour was not transformed into a number of points. It was used rather to calculate the outer bell surface area  $S_o$  applying again the Matlab program.

$$S_o = 2 \cdot \pi \cdot \sum_j (x_o - x_{out,j}) \cdot h, \quad (2)$$

where  $j$  denotes the number of pixels in the vertical direction ( $y$ ) from the top of the bell to its bottom,  $x_o$  is the horizontal position of the vertical symmetry axis of the bell,  $x_{out,j}$  denotes the position of the outer

contour at a specified vertical coordinate  $j$ ,  $h$  is the vertical height at each vertical position  $j$  and has therefore a value  $h = 1$  pix, which corresponds to the resolution of the image.

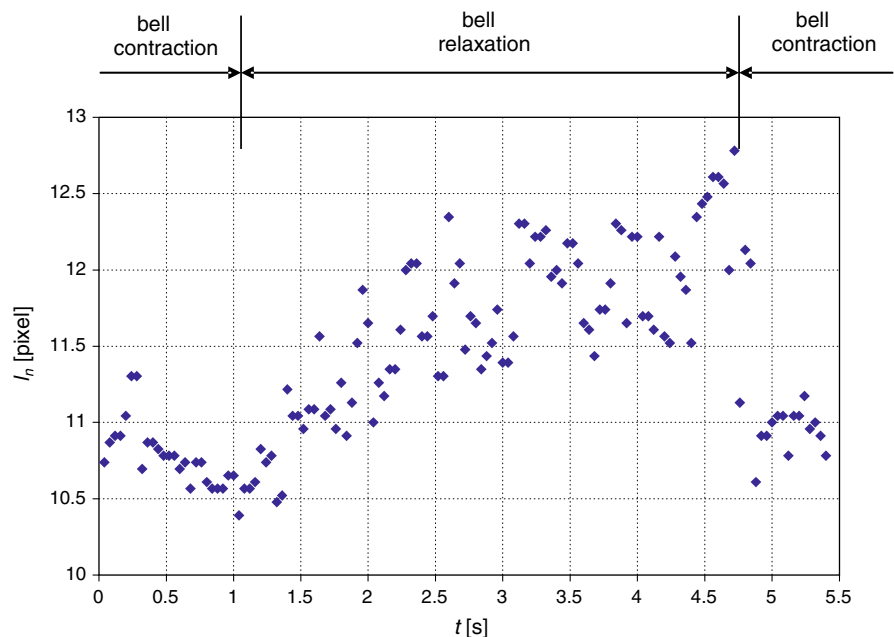
## Results

#### Movement of the exumbrellar contour

During the power stroke of the medusa (contraction), the average distance  $l_n$  (number of pixels) between two neighbouring points was generally up to 25% smaller than during the recovery stroke (relaxation). This indicated that there was either a certain level of stretching of the bell during relaxation or contraction during the power stroke; this is further investigated in the next section. The images were acquired at a fixed acquisition frequency; however, the power stroke was shorter than the recovery stroke (Fig. 5).

By processing the whole sequence of photographs, a time series of point coordinates was obtained (Fig. 6). All the selected points in Fig. 6 correspond to the points shown in Fig. 4b. The time series in Fig. 6a represent the horizontal movement of points on the bell contour, which was the result of both medusa displacement (i.e. the movement of the medusa's mass centre) and the relative movement

**Fig. 5** Average distance, in pixels, between two neighbouring points on the bell of the medusa for each image in the sequence



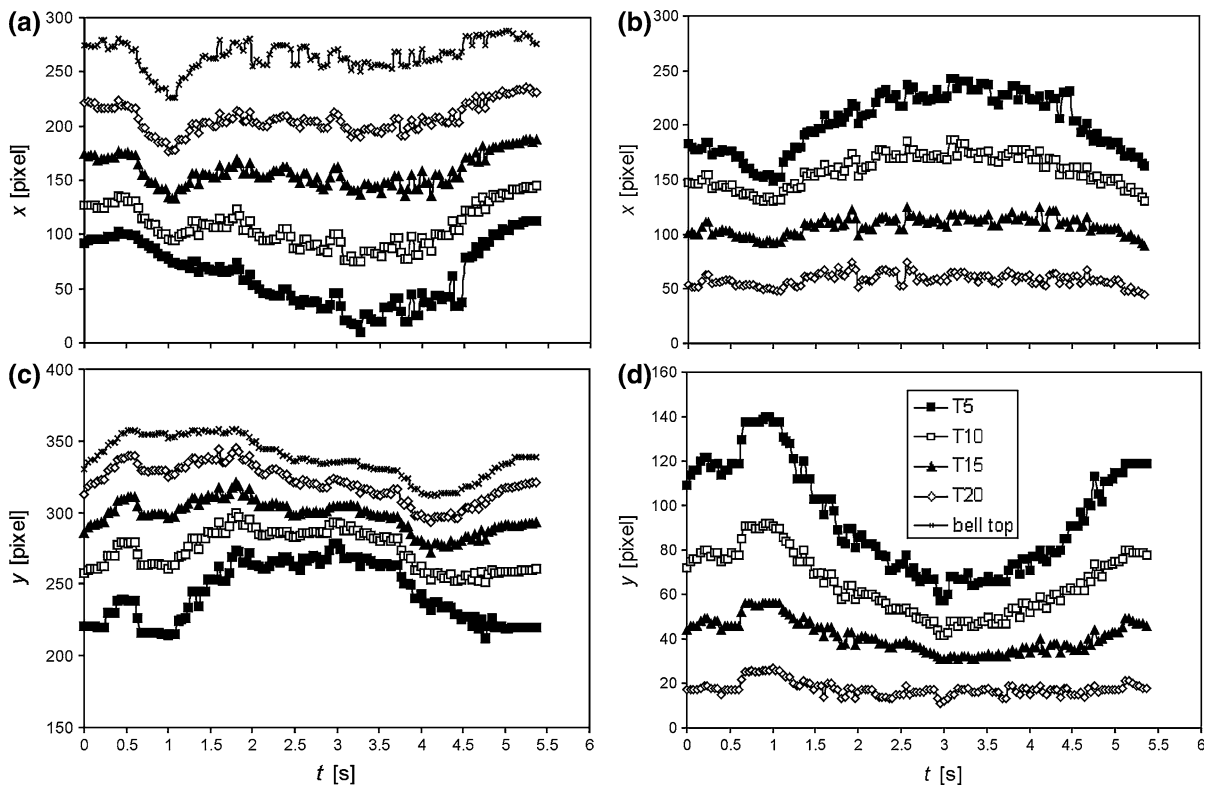


**Fig. 6** Time series of movement of the outer bell contour: (a) in  $x$ -direction (horizontal) for five different points on the outer contour of the medusa's bell; (b) in  $x$ -direction, relative to the

bell top (fixed point); (c) in the  $y$ -direction (vertical) for five points on the outer contour of the medusa's bell; (d) in  $y$ -direction, relative to the bell top (fixed point)

of the points with respect to the bell top, which was assumed to move in the  $x$ -direction only when the medusa as a whole moved in that direction. Time series of the movement of the points in the  $x$ -direction on the bell outer contour relative to the bell top are shown in Fig. 6b.

The lines in Fig. 6a and b are not smooth. This was most probably due to the error in calculating the position of a particular point, which had to be repeated for each image in the sequence. Such a procedure does not guarantee that the points are exactly equidistant.

A similar procedure can be applied to extract the time series of the point movement in the  $y$ -direction, as shown in Fig. 6c and d. Movement in both the  $x$ - and  $y$ -directions is more pronounced near the bell margin (e.g. points T5 and T10, Fig. 6b, d) than in the vicinity of the bell top (Fig. 6b, d). In this way, it is possible to compare the relative movement between arbitrary points chosen on the outer contour of the medusa's bell.

#### Changes of the bell surface area

Another sequence of images was used for determining alterations of the outer bell surface area during the bell pulsation cycle. This sequence was a little shorter than the first one and took less than 4 s to cover the complete pulsation cycle of the medusa. The area of the exumbrellar surface (i.e. the outer surface area of the bell) increased during relaxation and reached a maximum when the bell was in its most expanded state ( $t = \text{ca. } 2.5 \text{ s}$ , Fig. 7). The surface area of the outer bell at this point was ca. 1.34-fold greater than that at the state of maximum bell contraction ( $t = \text{ca. } 3.7 \text{ s}$ , Fig. 7).

#### Changes of the bell volume

Alterations in volume of the medusa and, in particular, the volume of subumbrellar space during the bell pulsation were further investigated. Here, the visualization method was again applied in order to

obtain the exumbrellar and the subumbrellar contours of the medusa’s bell from each image in the sequence, as shown in Fig. 3. The two contours confined the body of the medusa in a 2D image. Assuming axisymmetry of the bell movement, one curve for each half-contour was obtained for every image in the sequence (Fig. 8).

The bell volume between the exumbrellar and subumbrellar surfaces,  $V_{es}$  (depicted as two contours in a 2D diagram; Fig. 8), and the volume of the seawater in the subumbrellar cavity,  $V_w$ , were readily calculated for a particular image using Eqs. (3) and (4):

$$V_{es} = \pi \cdot \sum_j \left( (x_o - x_{out,j})^2 - (x_o - x_{in,j})^2 \right) \cdot h \tag{3}$$

$$V_w = \pi \cdot \sum_j (x_o - x_{in,j})^2 \cdot h, \tag{4}$$

where  $x_{in,j}$  denotes the position of the inner contour at a specified vertical coordinate  $j$ . Other quantities are the same as those specified in Eq. 2.

There was no significant change in bell volume between the exumbrella and subumbrella during a bell pulsation cycle (Fig. 9a). The dispersion of the results is nevertheless large; the highest values were ca. 1.2-fold greater than the lowest values. However, this could have resulted from the inherent uncertainty of the method, which was mainly due to the lighting

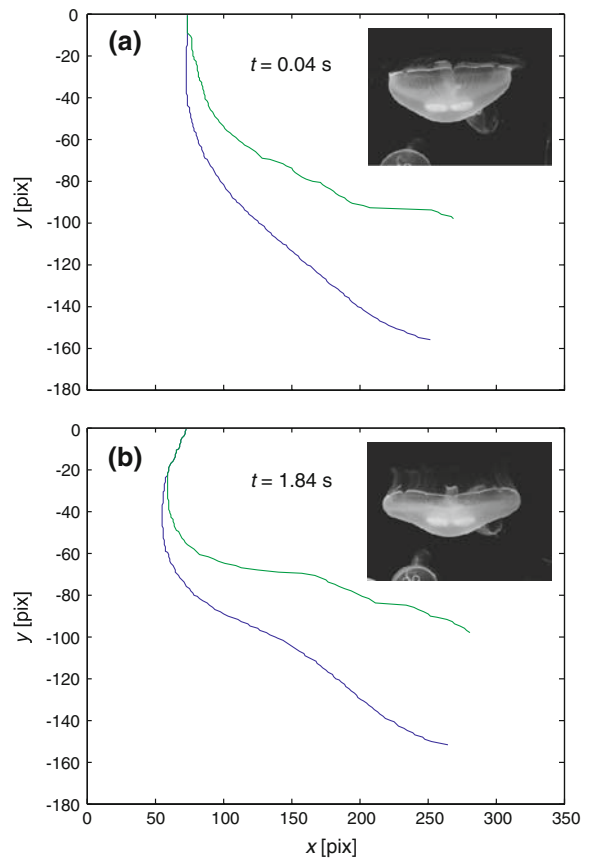


**Fig. 8** Outer and inner half-contours of the bell during phases of contraction (a) and relaxation (b) obtained by computer-aided visualization

**Fig. 7** Alterations of the outer surface area of the bell during a cycle of the bell pulsation

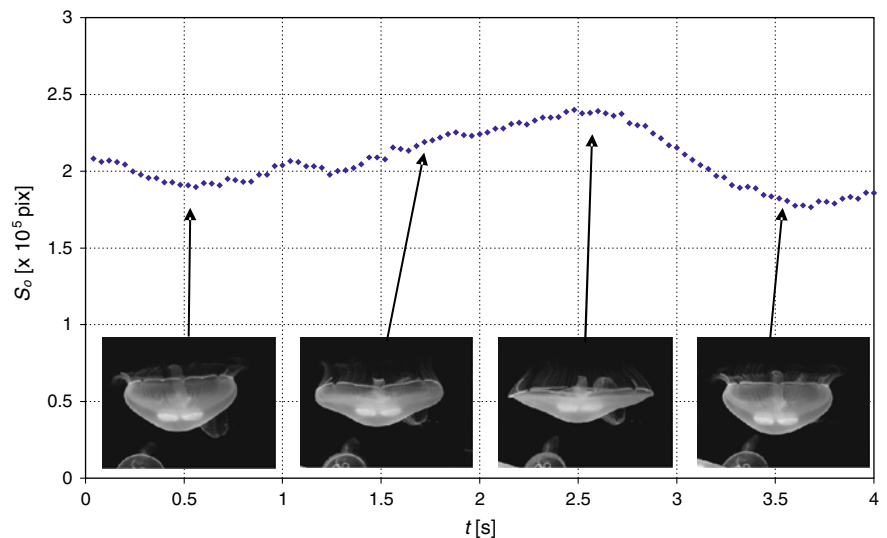
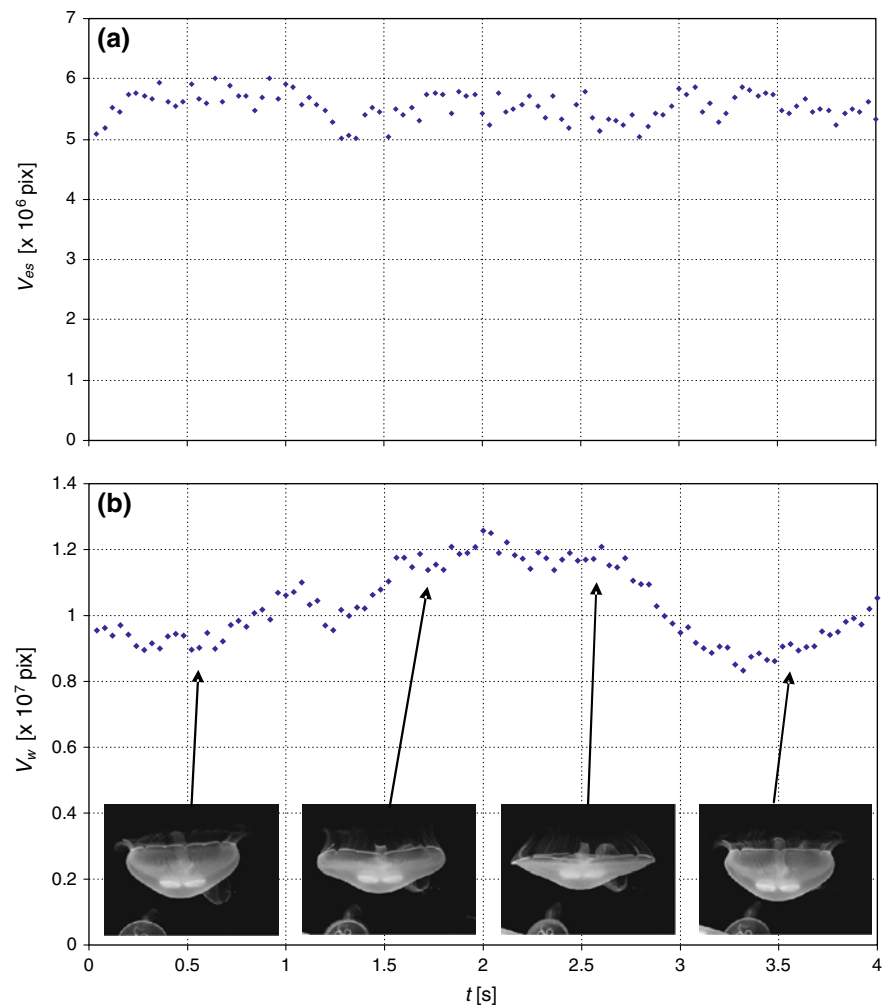


**Fig. 9** Volume during the pulsation cycle: (a) volume between the exumbrellar and subumbrellar (outer and inner) surfaces (bell volume); (b) volume of the water in the subumbrellar cavity



and hence the uncertainty of the inner bell contour at some places.

There was, however, a significant alteration in the subumbrellar cavity volume (i.e. the volume of fluid below the bell) (Fig. 9b). This was expected, since changes in this volume are needed to ensure propulsion of the medusa. The volume increased during the bell relaxation phase (time period between ca. 0.5–2.5 s, Fig. 9b). The ratio of the highest to the lowest values of the subumbrellar cavity volume was ca. 1.5.

The outer bell surface area ( $S_o$ ) and the volume of water in the subumbrellar cavity ( $V_w$ ) appeared to change in a similar way during the bell contraction cycle, since both diagrams (Figs. 7 and 9b) had a similar shape. Figure 10 shows the ratio between these two quantities ( $V_w/S_o$ ).

Both  $S_o$  and  $V_w$  were calculated from the same images. Although the laws governing the changing of

$S_o$  and  $V_w$  during the bell contraction cycle appeared to be similar, the ratio  $V_w/S_o$  was not constant (Fig. 10). The ratio increased when  $V_w$  increased. Detailed consideration of the evaluation of  $S_o$  and  $V_w$  showed, however, that there was a certain time delay between the calculated signals (i.e. between time series of  $S_o$  and  $V_w$ ). To estimate the time delay between  $S_o$  and  $V_w$ , the cross-correlation between the two signals was calculated using the following formula (Sach, 1997):

$$r(\Delta t) = \frac{\sum_i [(S_o(i + \Delta t) - \bar{S}_o) \cdot (V_w(i) - \bar{V}_w)]}{\sqrt{\sum_i (S_o(i + \Delta t) - \bar{S}_o)^2} \cdot \sqrt{\sum_i (V_w(i) - \bar{V}_w)^2}}, \quad (5)$$

where  $r$  denotes the cross-correlation coefficient (between 0 and 1),  $i$  is the current number of the

**Fig. 10** Ratio between the water volume in the subumbrellar cavity  $V_w$  and the exumbrellar surface area  $S_o$

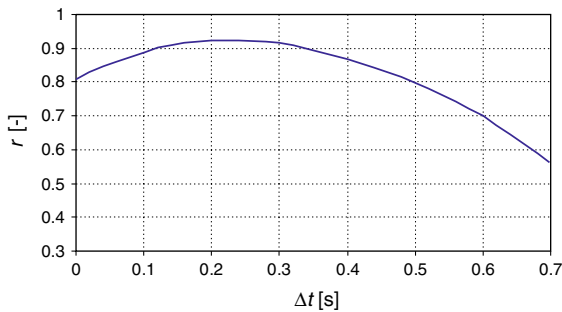
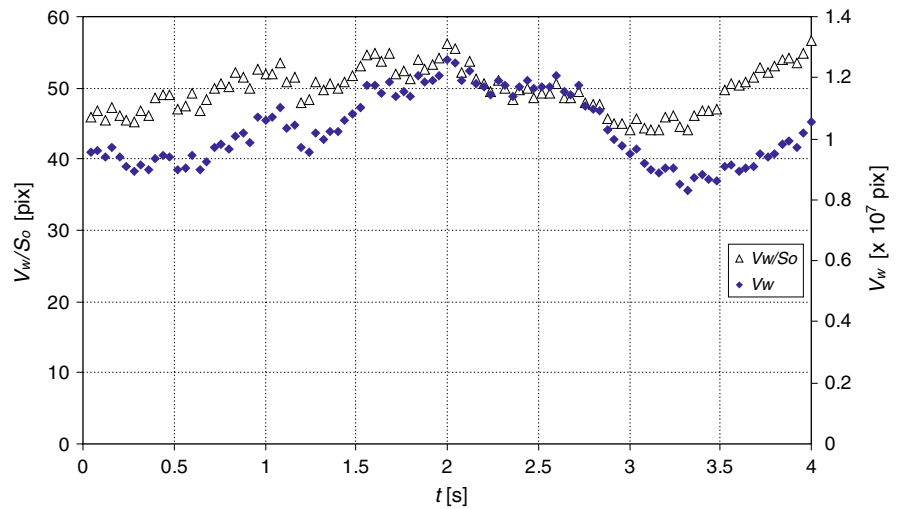


**Fig. 11** Correlation coefficient  $r$  for different time delays  $\Delta t$  between calculated time series of  $S_o$  and  $V_w$

image in the sequence and  $\bar{S}_o$  and  $\bar{V}_w$  denote the mean values of  $S_o$  and  $V_w$  over the whole sequence of  $i$  images.  $\Delta i$  is the sequence delay (i.e. the time delay  $\Delta t$ ) between series of  $S_o$  and  $V_w$ , where  $\Delta i = 0, 1, 2$ , etc. corresponds to the time delay  $\Delta t = 0$  s, 0.04 s, 0.08 s, respectively. The positive value of  $\Delta t$  means that  $S_o$  follows  $V_w$ .

The two time series were most closely correlated at a time delay of ca. 0.2 s, where the coefficient  $r$  had its maximum value of ca. 0.923 (Fig. 11). The change in exumbrellar surface area thus lagged behind the change in subumbrellar cavity volume by ca. 0.2 s.

**Discussion**

Kinematic characteristics of the scyphomedusa *Aurelia* sp. were obtained from reconstruction of

video images using a new, relatively simple computer-aided visualization. This method enabled us to examine changes in the medusa outer bell surface and the subumbrellar cavity volume in the course of a bell pulsation (contraction/relaxation) cycle. During the contraction phase, in addition to reduction of bell diameter (aperture), average distance between two neighbouring points on the outer bell surface decreased by up to 25%, most notably at the bell margin (i.e. Fig. 6). Similarly, Ford & Costello (2000) noted that in oblate hydrozoan genera bell contraction occurred primarily at the bell margin. While the bell volume between exumbrellar and subumbrellar surfaces (bell mesoglea) did not change significantly during the pulsation cycle, the ratio of the highest (relaxation) to the lowest (contraction) subumbrellar cavity volume amounted to about 1.5. The recoil phase during which the bell refills with water is accomplished by elastic energy stored in the mesoglea during bell contraction (DeMont & Gosline, 1988; Megill, 2002). Our analysis indicates that on average this phase lasts nearly twice as long as the contraction phase; this result is comparable to the values reported for *Aurelia* by Costello & Colin (1994) and found also for some other medusae species (Glatfelter, 1973; Ford et al., 1997; Shorten et al., 2005).

The bell radius (point T5 with respect to bell top, Fig. 6b)) oscillated with a range (peak-to-peak), which was about  $36 \pm 5\%$  of the maximum radius value ( $(90 \pm 10 \text{ pixels}) / (250 \pm 10 \text{ pixels})$ ). The relative change of the volume of the subumbrellar cavity with respect to the minimum cavity volume

was ca. 50%. This agrees well with the results of other investigators (Dabiri & Gharib, 2003), confirming again the reliability of the method.

Previous estimates of bell volume and the aperture area (Dabiri & Gharib, 2003) of jellyfish were grounded on insertion of a half-spline curve over the side image of jellyfish and the 3D bell was reconstructed by the revolution of a cubic spline around the axis of revolution. However, boundary points (pixels) on digital frames that separate the ambient fluid from the medusae bell have been selected by using the binary threshold filter with the conveniently set-up threshold level. The method here presented does not require this step. The boundary between the bell and the ambient is based on the exploration of the absolute gradients of pixels' intensity (Sobel, 1978), by sliding the  $3 \times 3$  convolution mask over the digital image and the threshold value of the gradient magnitude is much easier to set, since the gradients in intensities of pixels at the boundary are much larger than elsewhere. The same method was applied in this work exploring movements of bell parts along the length of the *Aurelia* bell. This differs from the method of Colin & Costello (2002) who made the morphological measurements of six co-occurring hydromedusae directly from video recordings calibrated with scale bars. Subsequently, they applied the same method to assess morphological traits of three upstream foraging medusae (Colin et al., 2006). Scale bars are not needed in the method presented here and our study demonstrates the ability of this approach to make better determinations of the bell shape parameters leading in turn to a better estimate of jellyfish dynamics. The major disadvantage of our fast method of image analysis lies in the relativity of scale: all space dimensions are scaled in pixels. As it was shown in this work, there are (nondimensional) quantities which could be successfully extracted with this method. Moreover, the pixel dimensions could be scaled with ingested objects of known dimensions (fluorescent beads).

## Conclusions

We have demonstrated a relatively simple method of analysing the shape of the bell of *Aurelia* sp. that leads to an estimate of the velocities of parts of the outer bell profile. The obtained results, such as the duration of power and recovery stroke, were in

agreement with the results of observations by other authors. This analysis also showed that alteration of the bell shape due to flexion, which conserves volume was a minor part of the bell's kinematics, while the changes of volume of the subumbrellar cavity play the dominant role during the relaxation/contraction of the bell. It can be concluded from the results of the analysis that the changes of subumbrellar cavity volume are manifested first by changes in the shape of the bell and second by changes in its outer surface area. These are, however, preliminary results that have to be further investigated.

It remains for the method presented here to be expanded on a larger population of *Aurelia* to confirm these interesting conclusions and to explore further how the swimming style is optimized according to the body size and shape. Knowledge of the kinematics of organisms with a complex shape is a prerequisite for the proper study of their dynamics, which is closely related to the hydrodynamics of the fluid that surrounds them. The latter will also be the focus of our future research.

## References

- Attrill, M. J., J. Wright & M. Edwards, 2007. Climate-related increases in jellyfish frequency suggest more gelatinous future for the North Sea. *Limnology & Oceanography* 52: 480–485.
- Brodeur, R. D., C. E. Mills, J. E. Overland, G. E. Walters & J. D. Schumacher, 1999. Evidence for a substantial increase in gelatinous zooplankton in the Bering sea, with a possible link to climate change. *Fisheries Oceanography* 8: 296–306.
- Colin, S. P. & J. H. Costello, 2002. Morphology, swimming performance and propulsive mode of six co-occurring hydromedusae. *The Journal of Experimental Biology* 205: 427–437.
- Colin, S. P., J. H. Costello & H. Kordula, 2006. Upstream foraging by medusae. *Marine Ecology Progress Series* 327: 143–155.
- Costello, J. H., S. P. Colin & J. O. Dabiri, 2008. Medusan morphospace: phylogenetic constraints, biomechanical solutions, and ecological consequences. *Invertebrate Biology*, doi:10.1111/j.1744-7410.2008.00126x.
- Costello, J. H. & S. P. Colin, 1994. Morphology, fluid motion and predation by the scyphomedusa *Aurelia aurita*. *Marine Biology* 121: 327–334.
- Costello, J. H. & S. P. Colin, 1995. Flow and feeding by swimming scyphomedusae. *Marine Biology* 124: 399–406.
- D'Ambra, I., J. H. Costello & F. Bentivegna, 2001. Flow and prey capture by the scyphomedusa *Phyllorhiza punctata* von Lendenfeld 1884. *Hydrobiologia* 451: 223–227.

- Dabiri, J. O., S. P. Colin & J. H. Costello, 2006. Fast-swimming hydromedusae exploit velar kinematics to form an optimal vortex wake. *Journal of Experimental Biology* 209: 2025–2033.
- Dabiri, J. O., S. P. Colin, J. H. Costello & M. Gharib, 2005. Flow patterns generated by oblate medusan jellyfish: field measurements and laboratory analyses. *Journal of Experimental Biology* 208: 1257–1265.
- Dabiri, J. O. & M. Gharib, 2003. Sensitivity analysis of kinematic approximations in dynamic medusan swimming models. *Journal of Experimental Biology* 206: 3675–3680.
- Daniel, T. L., 1983. Mechanics and energetics of medusan jet propulsion. *Canadian Journal of Zoology* 61: 1406–1420.
- DeMont, M. E. & J. M. Gosline, 1988. Mechanics of jet propulsion in the hydromedusan jellyfish, *Polyorchis penicillatus*. I. Mechanical properties of the locomotor structure. *Journal of Experimental Biology* 134: 313–332.
- Ford, M. D. & J. H. Costello, 2000. Kinematic comparison of bell contraction by four species of hydromedusae. *Scientia Marina* 64(Suppl 1): 47–53.
- Ford, M. D., J. H. Costello & K. B. Heilderberg, 1997. Swimming and feeding by the scyphomedusa *Chrysaora quinquecirrha*. *Marine Biology* 129: 355–362.
- Gladfelter, W. B., 1972. Structure and function of the locomotory system of the Scyphomedusa *Cyanea capitata*. *Marine Biology* 14: 150–160.
- Gladfelter, W. B., 1973. A comparative analysis of the locomotory systems of medusoid Cnidaria. *Helgolander wiss. Meeresunters* 25: 228–272.
- Graham, M., 2001. Numerical increases and distribution shifts of *Chrysaora quinquecirrha* (Desor) and *Aurelia aurita* (Linne) (Cnidaria: Scyphozoa) in the northern Gulf of Mexico. *Hydrobiologia* 451: 97–111.
- Graham, M., D. L. Martin, D. Felder, V. L. Asper & H. M. Perry, 2003. Ecological and economic implications of a tropical jellyfish invader in the Gulf of Mexico. *Biological Invasions* 5: 53–69.
- Hays, G. C., A. J. Richardson & C. Robinson, 2005. Climate change and marine plankton. *Trends in Ecology and Evolution* 20: 337–344.
- Lauder, G. V. & E. D. Tytell, 2006. Hydrodynamics of undulatory propulsion. *Fish Physiology* 23: 425–468.
- Malej, A. & A. Malej, 2004. Invasion of the jellyfish *Pelagia noctiluca* in the Northern Adriatic: a non-success story. In Dumont, H., T. Shiganova & U. Niermann (eds.), *Aquatic Invasions in the Black, Caspian, and Mediterranean Seas*. Kluwer Academic Press, Dordrecht: 273–285.
- Malej, A., V. Turk, D. Lučić & A. Benović, 2007. Direct and indirect trophic interactions of *Aurelia* sp. (Scyphozoa) in a stratified marine environment (Mljet Lakes, Adriatic Sea). *Marine Biology* 151: 827–841.
- Matanoski, J. C. & R. R. Hood, 2006. An individual-based numerical model of medusa swimming behaviour. *Marine Biology* 149: 595–608.
- Megill, W. M., 2002. The biomechanics of jellyfish swimming. Ph.D. Dissertation, Department of Zoology, University of British Columbia, 116 pp.
- Mills, C. B., 1981. Diversity of swimming behaviours in hydromedusae as related to feeding and utilization of space. *Marine Biology* 64: 185–189.
- Purcell, J. E. & M. N. Arai, 2001. Interactions of pelagic cnidarians and ctenophores with fish: a review. *Hydrobiologia* 451: 27–44.
- Sach, L., 1997. *Angewandte Statistik: Anwendung statistischer Methoden*. Springer-Verlag, Berlin.
- Shorten, M., J. Davenport, J. E. Seymour, M. C. Cross, T. J. Carrette, G. Woodward & T. F. Cross, 2005. Kinematic analysis of swimming in Australian box jellyfish, *Chiropsalmus* sp. and *Chironex flecheri* (Cubozoa, Cnidaria: Chirodropidae). *Journal of Zoology* 267: 371–380.
- Širok, B., T. Bajcar & M. Dular, 2002. Reverse flow phenomenon in a rotating diffuser. *Journal of Flow Visualization and Image Processing* 9: 193–210.
- Sobel, I., 1978. Neighborhood coding of binary images for fast contour following and general array binary processing. *Computer Graphics and Image Processing* 8: 127–135.